2003-02

Near-Surface Scintillation in the Marine Atmospheric Layer During the Red Field Campaign

Doss-Hammel, Stephen M.

P6.5 NEAR-SURFACE SCINTILLATION IN THE MARINE ATMOSPHERIC LAYER DURING THE RED FIELD CAMPAIGN

Stephen M. Doss-Hammel* and Dimitri Tsintikidis
Atmospheric Propagation Branch, SPAWAR Systems Center, San Diego, CA

Paul A. Frederickson and Kenneth L. Davidson
Department of Meteorology, Naval Postgraduate School, Monterey, CA

1. INTRODUCTION

Turbulence in the marine atmospheric surface layer can induce substantial perturbations in propagating infrared (IR) or optical signals. These perturbations result in scintillation, which is a fluctuation in received signal intensity. Scintillation can be quantified by the single parameter C_n^2, the refractive index structure parameter. It is necessary to measure C_n^2 from routine measurements in order to evaluate, predict, and compare EO system performance in operational environments and optimize EO systems for expected C_n^2 values from climatological measurements and models.

The Rough Evaporation Duct (RED) field test, conducted at Oahu, Hawaii, during August-September 2001, presented an excellent opportunity to quantify scintillation and to validate scintillation and transmission models.

We will comment on the progress toward the ultimate goals for this test. First, what is the influence of ocean waves on the near-surface propagation environment? The second goal is a determination of the accuracy of current C_n^2 estimation models for various ocean-atmosphere interaction scenarios including stable, near-neutral, and unstable conditions, and possible upgrade paths for the models.

2. THE INFRARED PROPAGATION EXPERIMENT

The field test was based upon measurements collected by a transmissometer system. The transmissometer consists of a broad-beam source coupled to a beam-forming telescope, and a receiving telescope connected to a data acquisition system. The broad-beam source comprised 18 halogen lamps modulated by a 690-Hz chopper wheel with a usable beam width exceeding 25°. The chopper signal is relayed to the receiver with a 162.1 MHz radio link. The receiver telescope has a primary mirror that is gold-plated paraboloid 20 cm in diameter and a focal length of 1.22 m (f/6).

The receiver system consisted of the telescope, a mid-wave infrared detector, and signal acquisition hardware. The detector is a non-imaging device cooled to 77°K. For a given source radiance the signal-noise ratio in the field is determined by the detector responsivity, noise density, and bandwidth. The mid-wave detector is a 2-mm diameter circular InSb photodiode mounted below a cold optical filter with an almost square band pass between 3.5 μm and 4.1 μm. The signal from the detectors is separated from the chopped carrier waveform by means of a lock-in amplifier system.

The infrared portion of the RED experiment was conducted on a propagation path approximately 10 km long connecting an IR broad-beam transmitter onboard R/V FLIP (13 m above waterline) and an IR telescope receiver at Malaekahana (3 m above ground) on the northeast coast of Oahu. The broad-beam source accommodated the pitch, roll, yaw, and translation of FLIP. The scintillation measurements were taken in the mid-wave (3.6 μm to 4.1 μm) every 15 minutes and at a 300 Hz sampling rate. Each measurement was 110 seconds long. Due to FLIP's tidal motion (±200 m in the NE-SW direction), hourly telescope alignments were necessary to ensure

* Stephen M. Doss-Hammel, Atmospheric Propagation Branch, SPAWAR Systems Center, Code 2858, San Diego, CA 92152; (619) 553-4578, email: hammel@spawar.navy.mil

proper signal reception. The data collection process occurred almost uninterruptedly for 16 continuous days.

The meteorological data were measured using the Naval Postgraduate School (NPS) `flux' buoy that was anchored approximately in the middle of the transmissometer path. The suite of meteorological instruments onboard the NPS flux buoy provided near-surface meteorology: air temperature, pressure, humidity (at various heights), wind speed and direction, sea surface temperature. In addition, air-sea fluxes and optical turbulence was measured. The NPS buoy meteorological data is a crucial element in the analysis of the transmission and scintillation time-series. Concurrent environmental measurements were obtained from a meteorological station mounted on top of a 30-ft mast outside the receiver station.

3. DATA ANALYSIS

There are two components of the infrared signal analysis. First we will utilize the abundant meteorological and surface flux measurements made during the test. The data from the mid-path meteorological buoy will be an essential part of this effort. The second component is a signal processing effort. The signal levels recorded from the field test are unexpectedly weak and it is meaningless to perform C_n^2 calculations using raw, unfiltered data. An approach to separate signal from noise without destroying the turbulent nature of infrared signal is necessary, and we will describe our use of a wavelet filtering scheme to attempt to accomplish the task.

The analysis of scintillation data for the RED test proved to be especially problematic. For transmission measurements the data acquisition mandated an averaging over a one minute interval, while the scintillation measurements required a 300 Hz sampling rate. Calculation of the expected free-space intensity for the system impelled us to set the voltage scale high enough to capture events at twice the free-space value of 1.02 mV. Almost all of the recorded data were below 0.4 mV. This compounded the usual noise problems by introducing digitization noise as well.

3.1 Wavelet Filtering

The intensity time-series data was filtered using a Daubechies wavelet filter (Daubechies 1992). Each scintillation data-set consisted of 2^{15} samples, collected at a 300 Hz rate. In the wavelet analysis the time-series data is transformed from 2^{15} signal amplitudes to 2^{15} wavelet coefficients.

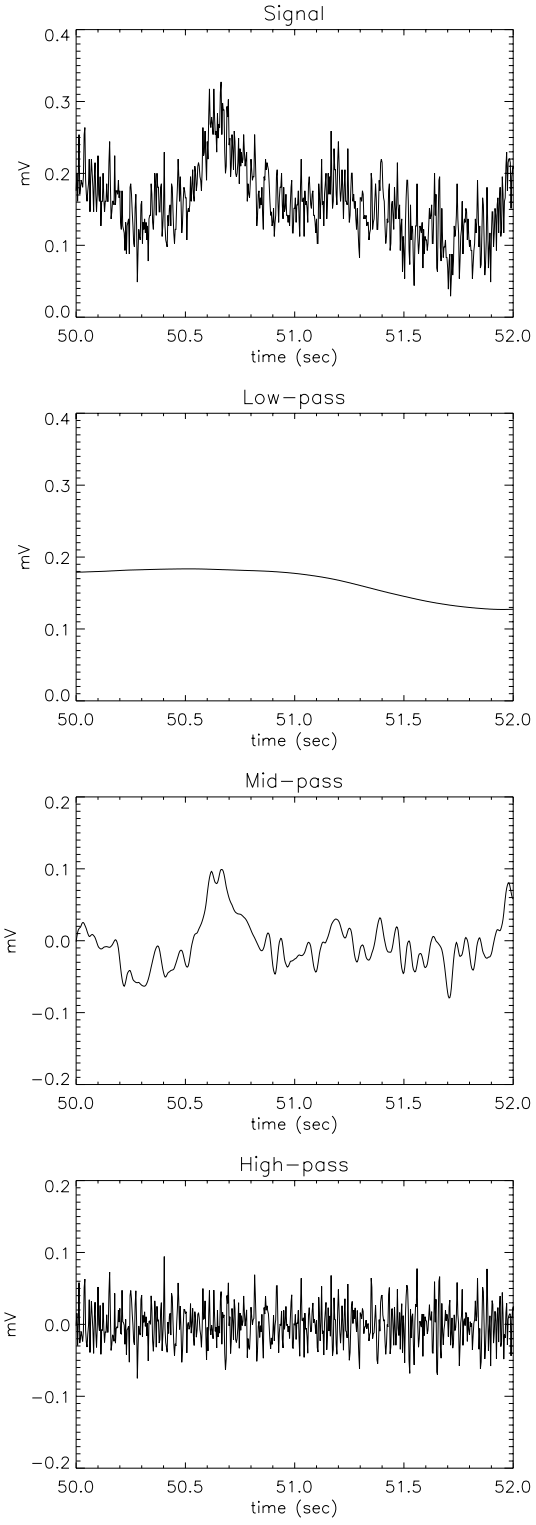

Figure 1: A 2-second infrared signal segment and the corresponding low-, mid-, and high-pass filtered components.

Each wavelet coefficient represents the correlation between a wavelet of a particular scale at a particular location in the time-series. For our data, there are 15 wavelet scales.

Our implementation of the wavelet transform generates a filter bank that trisects the data. After transforming to the wavelet scale space, two band cut-offs are selected, corresponding to a low-pass and a high-pass filter set, with a remaining middle band. The low-pass filter consisted of the six largest wavelet scales, and in frequency-space this roughly corresponded to all the data less than 1 Hz in frequency. The high-pass filter consists of the four smallest wavelet scales, and in frequency space these scales roughly represent the frequency components greater than 35 Hz.

The partition of the signal components into three bands is shown in Fig.1. The nature of the three bands can be seen in the figure with the unfiltered signal appearing in the uppermost panel. The second panel shows the low-pass band, which corresponds to the mean signal level and contains only low-frequency modulations of what is sometimes called the transmission value. The bottom panel, with the high-pass band, contains the high-frequency component. The high-pass band contains much of the system noise that accumulates in the data-analysis sequence. Finally, the mid-pass band contains the portion of the signal that generates most of the variance that is generated by scintillation effects for the full time-series.

3.2 Signal-Noise Ratio

The filtering process described above has been applied to previous field datasets (Doss-Hammel, 2002, and Tsintikidis, 2002) and for those cases, the amplitude of the high-frequency was substantially smaller than the amplitude of the mid-pass band. We have calculated the signal-noise ratio *SNR* for these filtering operations:

$$SNR = 10\log_{10}\left(\frac{\sigma^2_{mid}}{\sigma^2_{high}}\right) \qquad (1)$$

For most of our previous applications we have found that *SNR*>20. With a *SNR* at this level we can be assured that the mid-pass band contains almost all of the fluctuations induced by turbulence, and that the overall signal is not unduly contaminated by noise.

In this test, the signal quality was much poorer. As can be seen in fig. 1, we can no longer assume that the signal displayed in the mid-pass band is primarily due to turbulence-induced scintillation. The noise evident in the high-pass band must be assumed to contaminate the mid-pass band as well, and the noise contribution in that band is substantial. A signal with noise will generate a larger variance than the same signal without noise.

An additional problem with the C_n^2 calculation developed due to the geometry of the propagation path. The bearing of FLIP from the receiver site was 86°, and the sunrise azimuth varied from 80.4° to 86.8° over the fifteen-day test period. Solar glint into the receiver field of view increased the variance for approximately 3 hours after sunrise in each of the daily C_n^2 calculations.

A typical 24-hour record of *SNR* is shown in fig. 2. It is apparent that the *SNR* never exceeds 5 and that *SNR*<0 for the early morning solar interference part of the day.

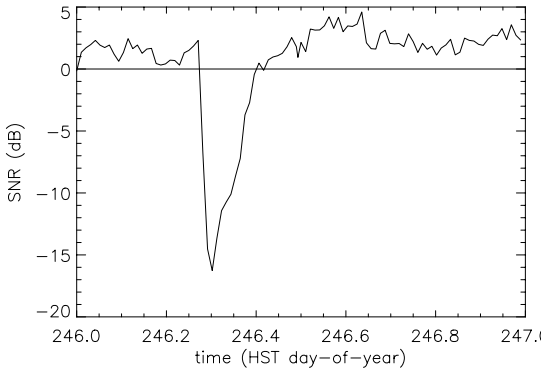

Figure 2: The signal-noise ratio in dB for the day 246 (shown in local time). Note that the solar interference in the morning sharply increases the noise level.

To calculate the infrared turbulence we determine C_n^2 using a saturation-resistant method (Hill 1978, Wang 1978):

$$C_n^2 = C_0 \sigma^2_{\ln I} D_t^{7/3} L^{-3} \qquad (2)$$

where L=10470 m is the propagation path length from transmitter to receiver; D_t is the transmitting aperture diameter; $\sigma^2_{\ln I}$ is the variance of the normalized log-intensity; and the factor C_0 is a function of the ratio between the receiver and transmitter apertures. The signal-noise ratio is a troublesome problem which we had not encountered in this severity during previous field experiments. The low values of *SNR* make any variance calculation for the last 5 days of the experiment unreliable. The calculations for the other days must be considered to be contaminated with some amount of noise: the measured infrared C_n^2 is lar-

ger than the true value. An indication of this problem can be seen in the comparison of three different determinations of C_n^2 in fig. 3.

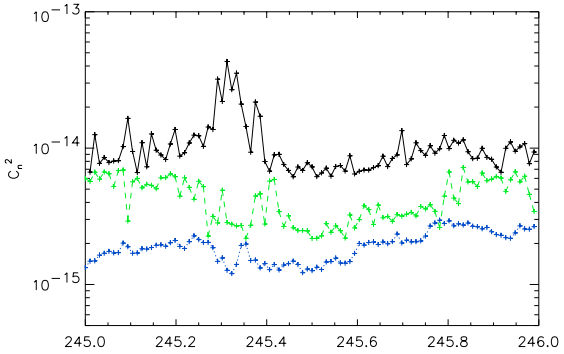

Figure 3: The refractive index structure parameter by three different methods: the top black line indicates the infrared signal measurement, the middle green dashed line is the direct turbulence measurement; the bottom blue line gives the bulk model estimate.

We have calculated the refractive index structure parameter C_n^2 three different ways (fig. 3). The uppermost black line shows the infrared signal measurement from the infrared transmission link, calculated with eqn. (2). The middle green dashed line is determined from the direct turbulence value from the sonic anemometers on the Naval Postgraduate School 'flux' buoy that was moored at the mid-point of the propagation path. Finally, the bottom blue line is computed from bulk C_n^2 estimates, developed from the relationship between mean parameters and turbulent fluxes. This calculation is based upon the Monin-Obhukhov surface layer similarity theory.

A similar comparison for data from previous field experiments resulted in a much better comparison between the infrared signal C_n^2 and the bulk C_n^2 calculations. This is another indication that the results from the infrared signal contain a large amount of noise.

4. CONCLUSIONS

The determination of the near-surface scintillation for the RED experiment was marred by an unexpectedly weak infrared signal. We are continuing to investigate the factors contributing to this small signal. We have indicated an example of the comparison between the infrared determination of C_n^2 and the determination by means of meteorological measurements along the propagation path. We believe that the infrared signal is inflated due to the presence of noise, and that the C_n^2 determination by means of direct turbulence measurements, or from mean measurements using mean models should be considered better estimates.

5. REFERENCES

Daubechies, I., 1992: "Ten Lectures on Wavelets", SIAM.

Doss-Hammel, S. and C. R. Zeisse, ``Refraction and scintillation in the atmospheric surface layer'', Proc. SPIE **4821**, 2002.

Hill, R. J. and R. G. Ochs, 1978: "Fine calibration of large-aperture optical scintillometers and an optical estimate of inner scale of turbulence." Applied Optics **17**, pp. 3608-3612.

Tsintikidis, D. and S. M. Doss-Hammel, ``Transmission and scintillation measurements for a summertime desert environment'', Proc. SPIE **4884**, 2002.

Wang, T.-I, G. R. Ochs, and S. F. Clifford, 1978: ``A saturation-resistant optical scintillometer to measure Cn2'', J. Opt. Soc. Am. 68, pp.334-338.